

# Quantum Linear Optics via String Diagrams

Giovanni de Felice and Bob Coecke

Quantinuum – Quantum Compositional Intelligence  
17 Beaumont street, OX1 2NA Oxford, UK

We establish a formal bridge between qubit-based and photonic quantum computing. We do this by defining a functor from the ZX calculus to linear optical circuits. In the process we provide a compositional theory of quantum linear optics which allows to reason about events involving multiple photons such as those required to perform linear-optical and fusion-based quantum computing.

## 1 Introduction

Quantum optics has pioneered experimental tests of entanglement [1], nonlocality [2], teleportation [3], quantum-key distribution [4], and quantum advantage [5]. These experiments ultimately rely on the ability to process coherent states of photons in *linear optical* devices, an intractable task for classical computers [6]. Recently, the potential of using linear optics for quantum computing has encouraged the development of both hardware [7] and software [8, 9] for photonic technologies. The first proposal was formulated by Knill, Laflamme and Millburn in 2001 [10]. Qubits are encoded in pairs of optical modes and quantum computing may be performed using only linear optical elements and photon detectors. Several improvements to the original scheme have been proposed in the literature [11, 12, 13]. Fusion measurements were introduced by Browne and Rudolf [14]. They form the basic ingredient of a recent proposal to achieve fault-tolerant quantum computation with photonic qubits [15].

String diagrams provide an intuitive language for quantum processes [16, 17, 18, 19, 20] and are implicitly employed in quantum software packages such as tket [21], PyZX [22], lambeq [23], DisCoPy [24], Quanhoven [25]. On the one hand, Coecke and Duncan [26] introduced the ZX calculus, a graphical language for reasoning about qubit quantum computing, with applications in circuit-based [27], measurement-based [28], and fault tolerant [29] quantum computing. The axioms of this calculus feature a bialgebra structure governing the Z and X qubit bases. On the other hand, Vicary and Fiore used the symmetric (or bosonic) Fock space to study the quantum harmonic oscillator, and discovered a different bialgebra structure on this infinite dimensional Hilbert space [30, 31]. These two foundational works are hardly ever related in the literature, possibly because of the difference in state space cardinality. However, it is well-known that photons in linear optics behave as quantum harmonic oscillators. Given the developments in linear-optical quantum computing, a formal bridge should be established between qubit-based and photonic QC. This would allow the construction of reliable software for compiling quantum computations into photonic circuits.

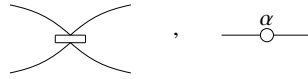
In this paper, we provide such a bridge by defining a functor from the ZX calculus to linear optics. In the process, we unify several results on the structure and combinatorics of quantum optical experiments. We start by studying the category of linear optical circuits, with their classical interpretation in terms of matrices or weighted paths (Sections 2). We then use the work of Vicary [30] to derive a functorial model for bosonic linear optics. Our first contribution is a proof that this model is equivalent to the model based on matrix permanents of Aaronson and Arkhipov [6] (Section 3). Second, we introduce a graphical calculus QPath which allows to compute the amplitudes of linear optical events involving multiple photons, by rewriting diagrams to normal form (Section 4). Finally, we construct a functor from

the ZX calculus to QPath and use it to describe the basic protocols used in linear-optical and fusion-based quantum computing (Section 5).

**Related work** Graphical approaches of linear optics are widespread in the literature. Notable examples are the matchgates introduced by Valiant [32], corresponding to fermionic linear optics [33], whose amplitudes are computed by finding the perfect matchings of a graph. Graph-theoretic methods are also widely used in bosonic linear optics [34, 35]. There are strong links between linear optics and categorical logic. Blute et al. [36] studied Fock space as exponential modality for linear logic. The fermionic version of the Fock space has been studied in [37], it forms the W core of the ZW calculus introduced by Coecke, Kissinger and Hadzihasanovic [38, 39, 40]. More recently, there has been work on a diagrammatic calculus for reasoning about polarising beam splitters for quantum control [41], an informal essay describing bosonic linear optics with category theory [42], and a complete rewriting system for the single photon semantics of linear optical circuits [43]. The ZX calculus has also been used to describe the fault-tolerant aspects of fusion-based quantum computing [44].

## 2 Linear optical circuits

Linear optical circuits are generated by two basic physical gates. The *beam splitter*  $\text{BS} : a \otimes a \rightarrow a \otimes a$  acts on a pair of optical modes, and may be implemented using prisms or half-silvered mirrors. The *phase shift*  $\text{S}(\alpha) : a \rightarrow a$  acts on a single mode and has a single parameter  $\alpha \in [0, 2\pi]$ . We depict them:



Linear optical circuits are obtained from these gates by composing them vertically and horizontally. They form a set **LO**, which has the structure of a free monoidal category, i.e. circuits can be composed in sequence or in parallel.

**Definition 2.1.** The classical interpretation of **LO** is given by a monoidal functor  $\mathcal{U} : \mathbf{LO} \rightarrow \mathbf{Mat}_{\oplus}$  into the category of matrices over the complex numbers, where  $\oplus$  is the direct sum of vector spaces. On objects  $\mathcal{U}$  is defined by  $\mathcal{U}(a) = \mathbb{C}$ . On arrows we have:

$$\mathcal{U}(\text{S}(\alpha)) = (e^{i\alpha})$$

$$\mathcal{U}(\text{BS}) = \frac{1}{\sqrt{2}} \begin{pmatrix} i & 1 \\ 1 & i \end{pmatrix}$$

where we use the standard interpretation of the beam splitter [45].

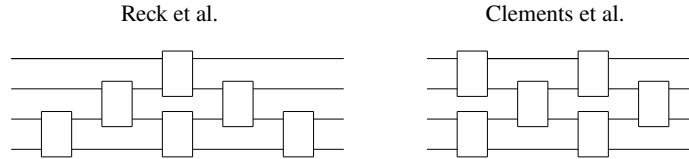
The Mach-Zender interferometer is obtained as the following composition:



The classical interpretation of this diagram is then given by:

$$\text{MZI}(\alpha, \beta) = ie^{i\alpha} \begin{pmatrix} -e^{i\beta} \sin(\alpha) & \cos(\alpha) \\ e^{i\beta} \cos(\alpha) & \sin(\alpha) \end{pmatrix}$$

MZIs may be used to parametrize any unitary map on  $m$  modes. They are the basic building blocks of integrated nanophotonic circuits currently being produced [7]. The first architecture for a universal multiport interferometer was proposed by Reck et al. [46] and consists of a mesh of MZIs. It was later simplified by Clements et al. into a grid-like architecture, reducing the depth from  $d = 2m - 3$  to  $d = m$  and thus the probability of photon loss [47].



Using one of these architectures, we have a parametrized circuit  $c(\theta) : m \rightarrow m \in \mathbf{LO}$ , where the parameters  $\theta$  correspond to phases  $\alpha, \beta$  of the Mach-Zender interferometers making up the chip. As shown in both [46] and [47], for any unitary  $U : \mathbb{C}^m \rightarrow \mathbb{C}^m$ , there is a configuration of parameters  $\theta$  such that  $\mathcal{U}(c(\theta)) = U$ . We may restate their results in our notation.

**Proposition 2.1** (Universality). [46, 47] *For any  $m \times m$  unitary  $U$ , there is a circuit  $c : m \rightarrow m$  in  $\mathbf{LO}$  such that  $\mathcal{U}(c) = U$ .*

In classical light experiments, we can measure the energy or *intensity* of an electromagnetic wave  $E = E_0 e^{i(kx - \omega t)}$  where  $k$  is the wavenumber,  $\omega$  is the angular frequency and  $E_0$  is called the amplitude [48]. The intensity is then given by the quadratic quantity  $I = \frac{c}{2} \epsilon_0 E_0^2$  where  $\epsilon_0$  is the permittivity of free space and  $c$  is the speed of light. The intensity is thus proportional to the Born rule  $I \propto \|E\|^2$ . Using the Born rule and the classical interpretation of  $\mathbf{LO}$ , we may compute the output distribution of a photonic chip  $c \in \mathbf{LO}$  with  $m$  spatial modes, when the input is a classical or *incoherent* beam of light. Suppose the input intensities of light are  $I \in \mathbb{R}^m$ . One may assume  $\sum_{i=1}^m I_i = 1$ . Then the intensities  $J$  at the output of an interferometer  $c \in \mathbf{LO}$  are given by:

$$J = \|\mathcal{U}(c)\|^2 I$$

where juxtaposition denotes matrix multiplication and the norm squared  $\|\cdot\|^2$  is applied entry-wise. Note that  $\|\mathcal{U}(c)\|^2$  is an invertible stochastic matrix since  $\mathcal{U}(c)$  is unitary.

**Example 2.1** (Classical light). *The intensities at the output of the beam splitter BS on any normalised input  $I$  are  $J = (\frac{1}{2}, \frac{1}{2})$  since:*

$$\|\text{BS}\|^2 = \begin{pmatrix} \frac{1}{2} & \frac{1}{2} \\ \frac{1}{2} & \frac{1}{2} \end{pmatrix}$$

*The Mach-Zender interferometer yields the following stochastic matrix:*

$$\|\text{MZI}(\alpha, \beta)\|^2 = \begin{pmatrix} \sin(\alpha)^2 & \cos(\alpha)^2 \\ \cos(\alpha)^2 & \sin(\alpha)^2 \end{pmatrix}$$

*The reflection and transmission coefficients for light intensities are given by  $R = \sin(\alpha)^2$  and  $T = \cos(\alpha)^2$  with  $R + T = 1$ . Thus, if we input a beam of incoherent light on the left leg  $I = (1, 0)$ , we will observe the distribution  $J = (R, T)$  in the output.*

We have seen that linear optical circuits have a classical interpretation as complex-valued matrices. We now give a graph-theoretic interpretation of these circuits, using a syntactic category for counting paths. The classical **Path** calculus has the following generators:

$$\begin{array}{c} \diagup \quad \diagdown \\ \diagdown \quad \diagup \end{array}, \quad \text{---} \circ, \quad \begin{array}{c} \diagdown \quad \diagup \\ \diagup \quad \diagdown \end{array}, \quad \circ \text{---}, \quad \begin{array}{c} \diagup \quad \diagdown \\ \diagdown \quad \diagup \end{array}, \quad \text{---}^r \quad (1)$$

denoted respectively  $\delta$ ,  $\epsilon$ ,  $\mu$ ,  $\eta$ ,  $\sigma$  and  $r$ . **Path** diagrams are obtained by composing these generators horizontally or vertically. Two **Path** diagrams are equal if we can rewrite from one to the other using the rules defined in Figure (1).

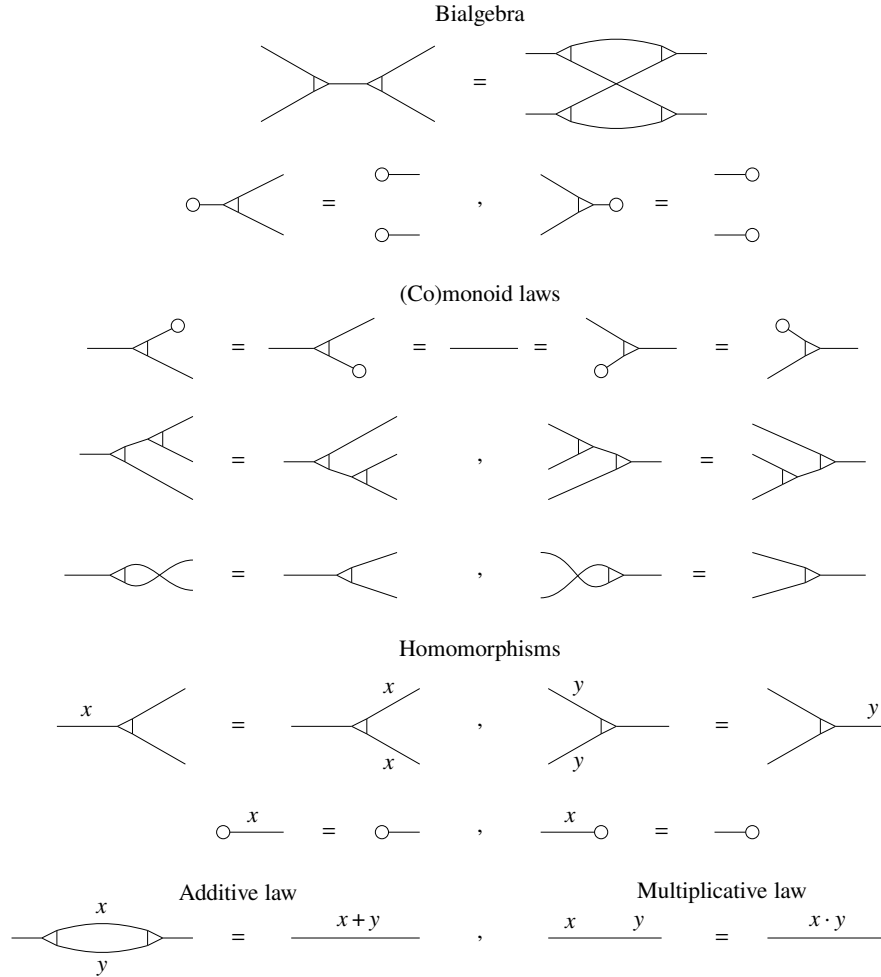


Figure 1: Axioms of the **Path** calculus

In categorical terms, we may define **Path** as the PROP generated by a bialgebra  $(\delta, \epsilon, \mu, \eta)$  together with endomorphisms  $r : 1 \rightarrow 1$  with a semiring structure  $r \in \mathbb{S}$ . Throughout this paper we fix  $\mathbb{S} = \mathbb{C}$  although our main results can be generalised to any semiring. We can interpret **Path** in the monoidal category of matrices with direct sum.

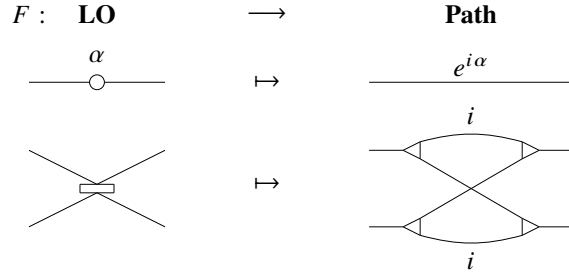
**Proposition 2.2.** *There is a monoidal functor  $C : \mathbf{Path} \rightarrow \mathbf{Mat}_{\oplus}$ .*

*Proof.*  $C$  is given on objects by  $C(a) = 1$  and on the generators (1) by:

$$C(\delta) = \begin{pmatrix} 1 & 1 \end{pmatrix}, \quad C(\epsilon) = () , \quad C(\mu) = \begin{pmatrix} 1 \\ 1 \end{pmatrix}, \quad C(\eta) = () , \quad C(r) = (r) , \quad C(\sigma) = \begin{pmatrix} 0 & 1 \\ 1 & 0 \end{pmatrix}.$$

where  $C(\mu) = () : 1 \rightarrow 0$  and  $C(\eta) = () : 1 \rightarrow 0$  are the unique morphisms of that type in  $\mathbf{Mat}_{\oplus}$ . It is easy to check that all the relations in Figure 1 are satisfied by  $C$ .  $\square$

Moreover, there is a functor turning linear optical gates into **Path** diagrams, representing their underlying matrix:

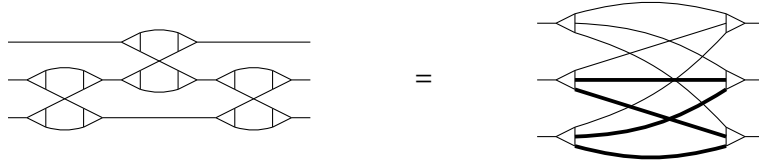


**Proposition 2.3.** *The classical interpretation of linear optics factors through the Path calculus, i.e. the functor  $F : \mathbf{LO} \rightarrow \mathbf{Path}$  defined above satisfies  $\mathcal{U} = F \circ C$ .*

The rewrite rules of **Path** allow to reduce any diagram to a normal form, which carries the same data as a weighted bipartite graph. This normal form can be reached by the following (pseudo) algorithm:

1. remove all instances of  $\eta : 0 \rightarrow 1$  and  $\epsilon : 1 \rightarrow 0$  by using the (co)unit and (co)copy laws repeatedly.
2. apply the bialgebra law and the multiplicative law until all instances of the comonoid  $\delta$  precede all instances of the monoid  $\mu$ ,
3. apply the additive rule to contract parallel edges.

As an example, the following equation holds in **Path**, the normal form procedure going from left to right.



where the thick wires carry the endomorphism  $2 : 1 \rightarrow 1$ . Computation of the weights on the resulting graph is equivalent to the block-diagonal matrix multiplication defined by  $C$ . This is stated formally as the following result.

**Proposition 2.4** (Completeness). *The axioms of **Path** are complete for  $\mathbf{Mat}_\oplus$ , i.e.  $C : \mathbf{Path} \rightarrow \mathbf{Mat}_\oplus$  is a monoidal equivalence.*

**Remark 2.1.** *This calculus is folklore and was popularised in a blog by Pawel Sobocinski on graphical linear algebra, however we don't know of any academic publication on the topic.*

### 3 Fock space and permanents

Processing bosonic particles, such as photons, with linear optical devices gives rise to statistics that are hard to simulate classically [6]. In this section we give an interpretation of linear optical circuits, derived from [30], in terms of free and symmetric Fock space functors  $\mathcal{F}, \mathcal{B} : \mathbf{Mat}_\oplus \rightarrow \mathbf{Vect}_\otimes$ . We show that this characterisation is equivalent to the model introduced in [6].

Consider a box containing particles. Assume that the space of states of a single particle is given by a Hilbert space  $H$ . The *free* Fock space is defined as follows:

$$\mathcal{F}(H) = \bigoplus_{n=0}^{\infty} H^{\otimes n}$$

where  $\otimes$  is the usual tensor product and  $\oplus$  the direct sum.  $\mathcal{F}(H)$  describes the state space of a given number of *distinguishable* particles indexed by  $n$ . Given a basis  $X$  of *modes* such that  $H = \mathbb{C}X$ , we have that  $\mathcal{F}(\mathbb{C}X) = l^2(X^*)$  where  $X^*$  is the set of lists of modes and  $l^2$  is the free Hilbert space construction [49]. Thus for  $n$  particles in  $m$  modes we have:

$$\mathcal{F}_n(\mathbb{C}^m) = (\mathbb{C}^m)^{\otimes n} \simeq \mathbb{C}([m]^n)$$

the basis states  $[m]^n$  are given by lists of length  $n$  using  $m$  distinct symbols.

**Proposition 3.1.** *The free Fock space can be extended to a functor  $\mathcal{F} : \mathbf{Mat}_\oplus \rightarrow \mathbf{Vect}_\otimes$  defined on arrows  $A : m \rightarrow k$  by:*

$$\mathcal{F}_n(A) = A^{\otimes n}$$

for  $n \in \mathbb{N}$ . Moreover it satisfies  $\mathcal{F}(A \oplus B) = \mathcal{F}(A) \otimes \mathcal{F}(B)$ .

*Proof.* This follows by functoriality and distributivity of tensor  $\otimes$  and biproduct  $\oplus$ .  $\square$

Now suppose that the particles in the box are *indistinguishable*. The state space of the system will then be described by the *symmetric* or bosonic Fock space, defined as follows:

$$\mathcal{B}(H) = \bigoplus_{i=0}^{\infty} H^{\hat{\otimes} i}$$

where  $\hat{\otimes}$  is the quotient of the tensor product by the equivalence relation  $x \hat{\otimes} y = y \hat{\otimes} x$ , which ensures that the bosons are indistinguishable. The  $n$ -particle sector of the bosonic Fock space  $\mathcal{B}_n(H)$  is simply the  $n$ -th component in the direct sum above. When  $H = \mathbb{C}^m$  is finite dimensional, we have  $n$  indistinguishable particles in  $m$  possible modes. The basis states of  $\mathcal{B}_n(H)$  are thus given by occupation numbers:

$$\Phi_{m,n} = \{ (s_1, \dots, s_m) \mid \sum_{i=1}^m s_i = n, s_i \in \mathbb{N} \}$$

Note that  $|\Phi_{m,n}| = \binom{m+n-1}{n}$  and  $\mathcal{B}_n(H) = H^{\hat{\otimes} n} = \mathbb{C}(\Phi_{m,n})$ . Let us compare the basis states for distinguishable and bosonic particles, there is a family of linear maps  $\alpha_H : \mathcal{F}(H) \rightarrow \mathcal{B}(H)$  defined on the basis states of the  $n$ -particle sector  $X \in [m]^n$  by:

$$\alpha(X) = \sqrt{\frac{n!}{\prod_{j=1}^m a(X)_j}} |a(X)\rangle$$

where  $a : [m]^n \rightarrow \Phi_{m,n}$  is defined by  $a(X)_j = |\{i \mid X_i = j\}|$  for  $j \in [m]$ . Note that the normalisation factor is equal to the size of the pre-image  $a^{-1}(a(X))$ . Let us write the map  $\alpha^\dagger$  explicitly:

$$\alpha^\dagger |I\rangle = \sqrt{\frac{N_I}{n!}} \sum_{X \in a^{-1}(I)} |X\rangle$$

where  $N_I = \prod_{j=1}^m \sqrt{I_j!}$ . We can now use  $\alpha$  to define the action of  $\mathcal{B}$  on arrows.

**Proposition 3.2.** [30] *The bosonic Fock space can be extended to a functor  $\mathcal{B} : \mathbf{Mat}_\oplus \rightarrow \mathbf{Vect}_\otimes$  defined on arrows  $A : m \rightarrow k$  by:*

$$\mathcal{B}_n(A) = A^{\hat{\otimes} n} = \alpha A^{\otimes n} \alpha^\dagger$$

and satisfying  $\mathcal{B}(A \oplus B) = \mathcal{B}(A) \otimes \mathcal{B}(B)$ .

*Proof.* This follows from  $\alpha^\dagger \circ \alpha = \text{id}$ , i.e.  $\alpha^\dagger$  is an isometry, see [30] for a general proof of this result.  $\square$

We can use the bosonic Fock space to define a functorial model for linear optics.

**Definition 3.1** (Functorial model). *The functorial interpretation of linear optics is given by the composition  $\mathcal{B} : \mathbf{LO} \xrightarrow{\mathcal{U}} \mathbf{Mat}_\oplus \xrightarrow{\mathcal{B}} \mathbf{Vect}_\otimes$ . Given a chip  $c : m \rightarrow m \in \mathbf{LO}$ , the probability of observing output state  $J \in \Phi_{m,n}$  on input  $I \in \Phi_{m,n}$  is given by:*

$$P_c^{\mathcal{B}}(J|I) = \|\langle J | \mathcal{B}(c) | I \rangle\|^2 = \|\langle J | \alpha \mathcal{U}(c)^{\otimes n} \alpha^\dagger | I \rangle\|^2$$

Aaronson and Arkhipov [6] introduced a formal model for linear optics based on the matrix permanent  $\text{Perm}$ .

**Definition 3.2** (Permanent model [6]). *Given a chip  $c : m \rightarrow m \in \mathbf{LO}$ , the probability of observing output state  $J \in \Phi_{m,n}$  on input  $I \in \Phi_{m,n}$  is given by:*

$$P_c(J|I) = \frac{1}{N_I N_J} \|\text{Perm}(\mathcal{U}(c)_{I,J})\|^2$$

where  $N_S = \prod_{j=1}^m S_j$ ,  $\text{Perm}$  denotes the matrix permanent, and  $U_{I,J}$  is the  $n \times n$  matrix obtained from the  $m \times m$  matrix  $U$  as follows. We first construct the  $m \times n$  matrix  $U_J$  by taking  $J_j$  copies of the  $j$ th column of  $A$  for each  $j \leq m$ . Then we construct  $A_{I,J}$  by taking  $I_i$  copies of the  $i$ th row of  $A_J$ .

We now prove the main result of this section.

**Theorem 3.1.** *The functorial model of linear optics is equivalent to the permanent model. Explicitly, for any  $m \times m$  unitary  $U$  and basis states  $I, J \in \Phi_{m,n}$*

$$\langle J | \mathcal{B}(U) | I \rangle = \frac{\text{Perm}(U_{I,J})}{\sqrt{N_I N_J}}$$

*Proof.* We start by expanding the left-hand side:

$$\begin{aligned} \langle J | \mathcal{B}(U) | I \rangle &= \langle J | U^{\otimes n} | I \rangle = \langle J | \alpha U^{\otimes n} \alpha^\dagger | I \rangle = (\alpha^\dagger | J \rangle)^\dagger U^{\otimes n} (\alpha^\dagger | I \rangle) \\ &= \left( \sqrt{\frac{N_J}{n!}} \sum_{Y \in a^{-1}(J)} \langle Y | \right) U^{\otimes n} \left( \sqrt{\frac{N_I}{n!}} \sum_{X \in a^{-1}(I)} | X \rangle \right) \\ &= \frac{\sqrt{N_J N_I}}{n!} |a^{-1}(I)| \sum_{Y \in a^{-1}(J)} \langle Y | U^{\otimes n} | \hat{X} \rangle \\ &= \frac{\sqrt{N_J N_I}}{n!} \frac{n!}{N_I N_J} \sum_{\sigma \in S_n} \prod_{i=1}^n U_{\hat{X}_i, \hat{Y}_{\sigma(i)}} \\ &= \frac{1}{\sqrt{N_I N_J}} \text{Perm}(U_{I,J}) \end{aligned}$$

where  $\hat{X} \in a^{-1}(I)$  and  $\hat{Y} \in a^{-1}(J)$  are any chosen representatives. Note that this choice is irrelevant since we sum over all permutations, and so in particular we can set  $(U_{I,J})_{ij} = U_{\hat{X}_i, \hat{Y}_j}$ , yielding the last step.  $\square$

**Example 3.1** (Hong-Ou-Mandel). *Consider the matrix of the beam splitter:*

$$U = \frac{1}{\sqrt{2}} \begin{pmatrix} i & 1 \\ 1 & i \end{pmatrix}$$

*Suppose we input one boson in each port  $I = (1, 1)$ . There are three possible outcomes  $J = (2, 0), (1, 1), (0, 2)$ . We may determine the amplitudes of the different outcomes by computing permanents:*

$$\text{Perm} \begin{pmatrix} i & i \\ 1 & 1 \end{pmatrix} = 2i \quad \text{Perm} \begin{pmatrix} i & 1 \\ 1 & i \end{pmatrix} = 0 \quad \text{Perm} \begin{pmatrix} 1 & 1 \\ i & i \end{pmatrix} = 2i$$

*The component for outcome  $(1, 1)$  is 0. We deduce that the probability of observing one boson in each output port is 0. Thus interference ensures that the bosons bunch together at the output of the device, a phenomenon known as the Hong-Ou-Mandel effect.*

## 4 Quantum paths and matchings

In the previous section we have shown that bosonic linear optics can be formulated equivalently in terms of Fock space and permanents. Aaronson and Arkhipov [6] used the second definition to show that sampling from a linear optical chip with bosonic particles is classically hard: if a classical computer can compute an additive approximation of matrix permanents then the polynomial hierarchy collapses. While this computational definition is useful for proving complexity results about linear optics, we want to develop a diagrammatic syntax for *programming* linear optical circuits. We do this by developing a quantised calculus **QPath** which allows us to compute the amplitudes of linear optical events involving multiple photons, using simple rewrite rules. In order to quantise the **Path** calculus, we add creation and annihilation of particles as generators.

$$\mathbf{QPath} = \mathbf{Path} + \left\{ \begin{array}{c} |n\rangle \\ \bullet \text{---} \end{array}, \quad \text{---} \bullet \begin{array}{c} |n\rangle \end{array} \right\}_{n \in \mathbb{N}^+}$$

This yields a free monoidal category where we can represent linear optical processes with state preparations (creation) and post-selection (annihilation). Before developing a calculus around the **QPath** generators, the first thing to note is that **QPath** is equivalent to **Path** if we interpret it in classically, i.e. functors  $\mathbf{QPath} \rightarrow \mathbf{Mat}_\oplus$  are in bijective correspondence with functors  $\mathbf{Path} \rightarrow \mathbf{Mat}_\oplus$ . In fact, black and white nodes are necessarily equal in  $\mathbf{Mat}_\oplus$ , since the unit 0 of  $\oplus$  is both a terminal and an initial object. In order to interpret black nodes, representing modes occupied by photons, we need to use the bosonic Fock space functor.

The quantum interpretation  $\mathcal{B} : \mathbf{QPath} \rightarrow \mathbf{Hilb}_\otimes$  is obtained on the generators (1) by composing  $C : \mathbf{Path} \rightarrow \mathbf{Mat}_\oplus$  with the bosonic Fock space functor  $\mathcal{B} : \mathbf{Mat}_\oplus \rightarrow \mathbf{Hilb}_\otimes$ . The generating object  $a$  of **QPath** is mapped to the free Hilbert space  $l^2(\mathbb{N})$ . The comonoid  $\delta : 1 \rightarrow 2$  is mapped as follows:

$$\begin{array}{c} \diagup \\ \text{---} \triangleleft \\ \diagdown \end{array} \mapsto \mathcal{B}(\delta) : |n\rangle \mapsto \sum_{k=0}^n \binom{n}{k}^{\frac{1}{2}} |k\rangle |n-k\rangle,$$

while the monoid  $\mu$  is mapped to the *dagger*  $\mathcal{B}(\mu) = \mathcal{B}(\delta)^\dagger$ . White nodes are mapped to  $|0\rangle, \langle 0|$ , indicating that the mode is empty. Endomorphisms  $r : 1 \rightarrow 1$  in **QPath** are interpreted as follows:

$$\text{---} \overset{r}{\text{---}} \mapsto \mathcal{B}(r) : |n\rangle \mapsto r^n |n\rangle$$



Finally, the black nodes in **QPath** are mapped respectively to  $|n\rangle$  and  $\langle n|$ , indicating that the mode is occupied by  $n$  particles. Hadzihasanovic [40] showed directly that  $(\mu, |0\rangle, \delta, \langle 0|)$  forms a bialgebra. In fact all the axioms that hold in the classical interpretation  $\mathcal{C}$  also hold in the bosonic interpretation  $\mathcal{B}$  since it is defined by functor-composition. However, black nodes allow to express some processes which were not available in the classical semantics, as we will see below.

The axioms of **QPath** include all the axioms of **Path**, given in Figure 1. The only additional rules we will need to reason with black nodes are the following:

$$\begin{array}{c}
 \text{Scalar} \qquad \qquad \qquad \text{Bone} \\
 \bullet \xrightarrow{r} \bullet = r \qquad , \qquad \bullet \circ = 0 = \circ \bullet \qquad , \\
 \\
 \text{Branching} \\
 \begin{array}{ccc}
 \bullet \text{---} \triangleleft \begin{array}{l} \diagup \\ \diagdown \end{array} & = & \begin{array}{cc} \circ \text{---} & \bullet \text{---} \\ \bullet \text{---} & \circ \text{---} \end{array} + , \qquad \begin{array}{l} \diagup \\ \diagdown \end{array} \triangleleft \bullet & = & \begin{array}{cc} \text{---} \circ & \text{---} \bullet \\ \text{---} \bullet & \text{---} \circ \end{array} + \\
 \end{array} \\
 \\
 \text{Normalisation} \\
 \sqrt{n!} \begin{array}{c} \bullet \text{---} \\ |n\rangle \end{array} = \begin{array}{c} \bullet \\ \vdots n \\ \bullet \end{array} \triangleleft \text{---} , \qquad \text{---} \begin{array}{c} \bullet \\ |n\rangle \end{array} \sqrt{n!} = \text{---} \triangleleft \begin{array}{c} \bullet \\ n \vdots \\ \bullet \end{array}
 \end{array}$$

Figure 2: Additional axioms for the **QPath** calculus

It is easy to show that the axioms above are sound for the bosonic interpretation  $\mathcal{B}$ .

**Example 4.1** (Creation/Annihilation). *The creation and annihilation operators on single modes have the following representation as QPath diagrams.*

*Creation*                      *Annihilation*

We recover the commuting relations for these operators using the branching law:

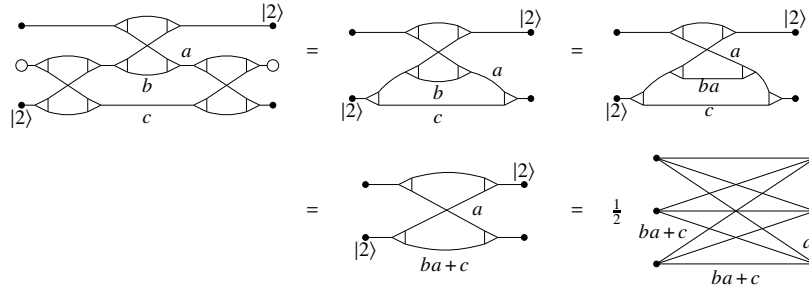
**Example 4.2** (Hong-Ou-Mandel). We compute the amplitude of the beam splitter BS on input/output  $I = (1, 1) = J$ :

$$\begin{array}{c} i \\ \text{---} \text{---} \text{---} \\ \text{---} \text{---} \text{---} \\ i \end{array} = \begin{array}{c} i \\ \text{---} \text{---} \end{array} + \begin{array}{c} \text{---} \text{---} \\ \text{---} \text{---} \end{array} = -1 + 1 = 0$$

and we recover the zero amplitude for this event.

We interpret a *closed* diagram  $d : 0 \rightarrow 0 \in \mathbf{QPath}$  as an event where particle creations are matched to particle annihilations. Given a linear optical circuit  $c : m \rightarrow m \in \mathbf{LO}$  together with a pair of states  $I, J \in \Phi_{m,n}$  of occupation numbers, we may construct a closed diagram  $d = \langle I | F(c) | J \rangle \in \mathbf{QPath}$ , corresponding

to the event that we observe output  $J$  when we input  $I$  in a chip  $c$ . Using only the **Path** axioms together with the normalisation rule, we can rewrite  $d$  as in the following example.



where we use the following syntactic sugar:  $\langle := \bullet \rightarrow \bullet$ ,  $\rangle := \bullet \leftarrow \bullet$ . At the end of the rewriting process, we obtain a weighted bipartite graph. Let us denote this graph by  $G_d = (N, E)$  where  $N$  is the set nodes and  $E \subseteq N^2$  is the set of edges, together with  $w : E \rightarrow \mathbb{C}$  an assignment of complex weights to every edge. Note that  $G$  is an undirected graph, i.e.  $(i, j) \in E \implies (j, i) \in E$ .

**Proposition 4.1** (Normal form). *Any closed diagram  $d \in \mathbf{QPath}$  can be reduced to a pair  $(G_d, N_d)$ , where  $G_d$  is weighted bipartite graph and  $N_d$  is a normalisation factor, using the axioms in Figure 1 and the normalisation law.*

*Proof.* The normal form procedure exemplified above is the same as for **Path**, with the addition of the use of the normalisation law which determines  $N_d$ .  $\square$

Once  $d \in \mathbf{QPath}$  has been reduced to a weighted bipartite graph, we may further reduce it down to a scalar value by using the branching and scalar laws. Most terms obtained by branching will cancel out because of the first scalar law. The remaining terms are found to be in one-to-one correspondence with the *perfect matchings* of  $G_d$ . Recall that a matching for a graph  $G$  is a subset of the edges  $M \subseteq E$  such that no node is contained in two edges of  $M$ . A perfect matching is a matching  $M$  such that every node is contained in an edge of  $M$ .

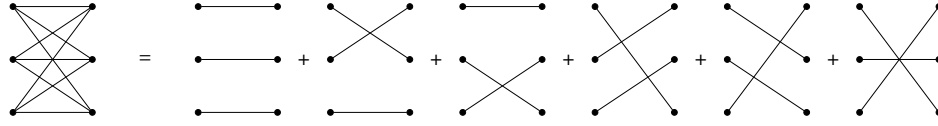
**Theorem 4.1** (Completeness). *For closed diagrams  $d : 0 \rightarrow 0 \in \mathbf{QPath}$ , the rewrite rules of **QPath** are complete for the bosonic interpretation  $\mathcal{B} : \mathbf{QPath} \rightarrow \mathbf{Hilb}_{\otimes}$ , which moreover satisfies:*

$$\mathcal{B}(d) = N_d \sum_M \prod_{e \in M} w_e \quad (2)$$

where  $M$  ranges over the perfect matchings of the graph  $G_d$ .

*Proof.* We need to show that if two closed diagrams  $d, d'$  have the same interpretation  $\mathcal{B}(d) = \mathcal{B}(d') \in \mathbb{C}$ , then we can rewrite from  $d$  to  $d'$  using the axioms of **QPath**. To see this, note that for any closed diagram  $d$ , the branching law turns the graph  $G_d$  into a sum of  $n^n$  terms, where  $n$  is the number of photon preparations. We can cancel most of these terms using the “bone” law, which leaves us with  $n!$  terms corresponding to the perfect matchings of  $G_d$ : each photon preparation is matched to a photon annihilation. Finally we reduce each of the terms to a complex value using the scalar law. It is a standard result in graph theory that the sum of weights of perfect matchings of a graph is equal to the permanent of its adjacency matrix, yielding (2). Therefore we can use the axioms of **QPath** to reduce both  $d$  and  $d'$  to the same scalar value in  $\mathbb{C}$ . Since all the rules of **QPath** are invertible we can rewrite from  $d$  to  $d'$ , yielding completeness. We do not currently know if the rules are complete also for “open” diagrams.  $\square$

**Example 4.3.** For a generic event  $d$  with three photons in **QPath**, the normal form procedure gives us a weighted bipartite graph  $G_d$  with input and output of size 3, or equivalently we have a  $3 \times 3$  adjacency matrix of weights. Using the branching law, we reduce the diagram to the following sum:

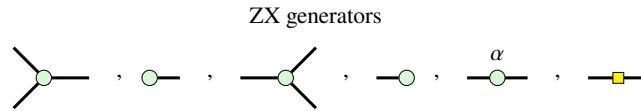


equivalently, we have just split the graph into its perfect matchings. Now we use the scalar laws to reduce each term to a complex number. Equivalently, we multiply the weights assigned to the edges on each matching. Finally we sum those terms to obtain the amplitude. Equivalently, we have computed the permanent of the adjacency matrix of  $G_d$ .

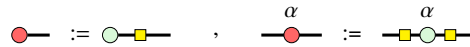
## 5 Linear-optical quantum computing

Our aim in this section is to describe how linear optics is used for qubit quantum computation. We will do this by giving a complete mapping from the **ZX** calculus to **QPath**. We start by introducing the **ZX** calculus on qubits. The dual-rail encoding allows to encode a logical qubit as a photon in a pair of spatial modes. We show how all single qubit unitaries may be applied using simple linear optical devices. We describe fusion measurements as diagrams in **QPath** and show how they can be used, along with polarising beam splitters, to construct Bell states and more general cluster states.

**ZX calculus.** The **ZX** calculus is a graphical language for reasoning about qubit quantum computation. It has strong links with both circuit-based and measurement-based models of quantum computing [28]. The **ZX** calculus is generated by the following basic operations:

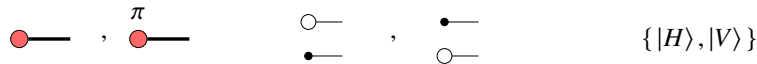


We will also use the following syntactic sugar for **X** states and phases:

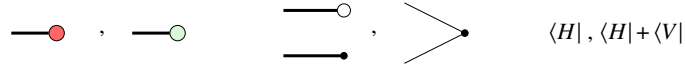


In this section we are not really interested in the rewrite rules for **ZX** diagrams, rather in their interpretation as linear maps between qubits. We will give this interpretation as we map each **ZX** generator to post-selected optical circuits in **QPath**, and refer to [50, 20] for more in-depth discussions.

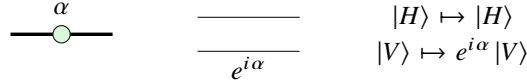
**Dual rail qubits.** The dual-rail encoding can be thought of as a translation between polarized and spatial modes of photons. The polarization states of a single photon are spanned by the basis states  $|H\rangle, |V\rangle$  for horizontal and vertical polarization, and thus naturally form a *qubit*. The dual-rail encoding consists in encoding a polarised mode of light as a pair of spatial modes in **LO** under the mapping  $|H\rangle \mapsto |0, 1\rangle, |V\rangle \mapsto |1, 0\rangle$ . The **Z** basis of a dual rail qubit may be expressed as a pair of **QPath** diagrams:



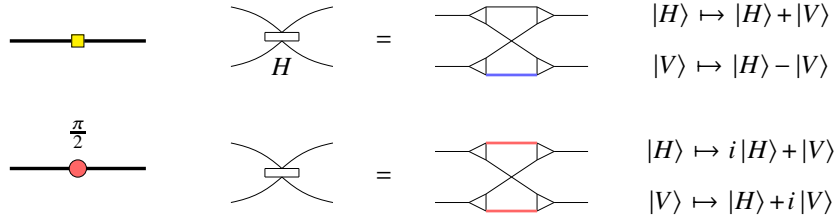
The  $Z$  and  $X$  effects correspond to the following diagrams:



The  $Z$  effect may be implemented by post-selecting a photon detector, the  $X$  effect by precomposition with a beam splitter.  $Z$  phases on dual-rail qubits are obtained as follows:

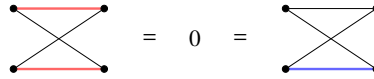


The rotations  $BS_X$  and  $BS_Y$  from the  $Z$  basis to the  $X$  and  $Y$  bases are given by the following beam splitters:

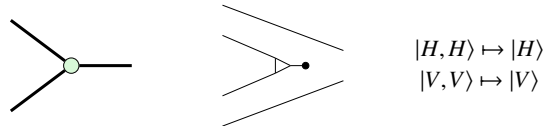


where we use the syntactic sugar:  $\text{blue line} := -1$ ,  $\text{red line} := i$ . In particular, the hadamard gate corresponds to  $BS_H$ . We may obtain all single qubit unitaries in dual rail encoding using  $Z$  phases and either  $BS$  or  $BS_H$ .

**Example 5.1 (HOM).** Using the beam splitters above, we obtain two versions of the Hong-Ou-Mandel effect which are depicted graphically as follows:

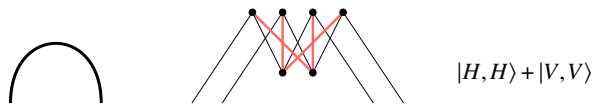


**Fusion measurements.** Fusion measurements are Bell measurements on dual-rail qubits. They correspond to the linear map:  $|H, H\rangle \mapsto |H\rangle$ ,  $|V, V\rangle \mapsto |V\rangle$ ,  $|H, V\rangle, |V, H\rangle \mapsto 0$ , which is denoted as a green spider with two inputs and one output in **ZX**, and is obtained on dual-rail qubits as the following diagram in **QPath**.

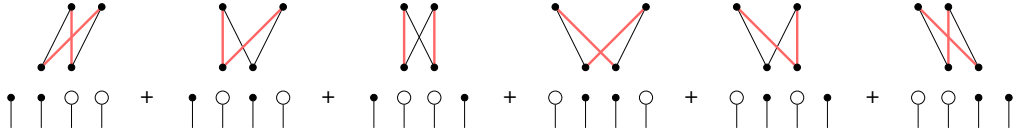


To see that this measures the Bell basis, note that there must be exactly one photon in the two middle modes. The input basis state in dual-rail encoding are  $\{|0101\rangle, |0110\rangle, |1010\rangle, |1001\rangle\}$  and this condition is satisfied only by  $|1010\rangle$  and  $|0101\rangle$  which correspond respectively to  $|H, H\rangle$  and  $|V, V\rangle$ .

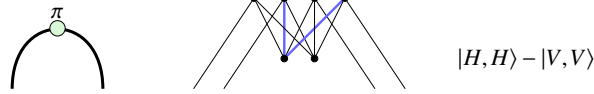
**Bell states.** We engineer a representation of dual-rail bell states as **QPath** diagrams.



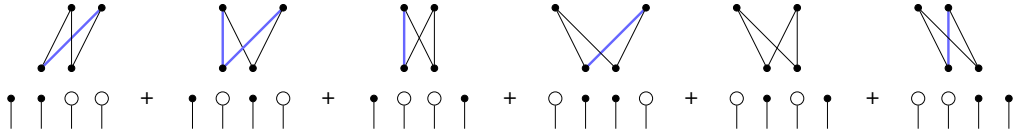
We can check that this diagram corresponds to the bell state  $|H, H\rangle + |V, V\rangle$  by branching:



and using the Hong-Ou-Mandel effect (Example 5.1). Similarly, the Bell state  $|HH\rangle - |VV\rangle$  may be represented using blue edes as follows:

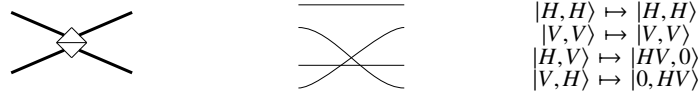


and we can check this using branching and HOM:

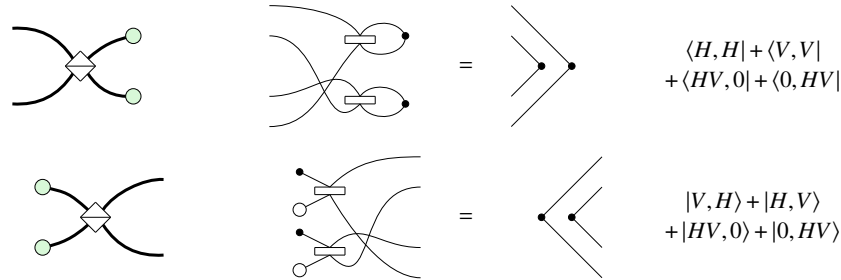


Note that there may be different equivalent representations of Bell states.

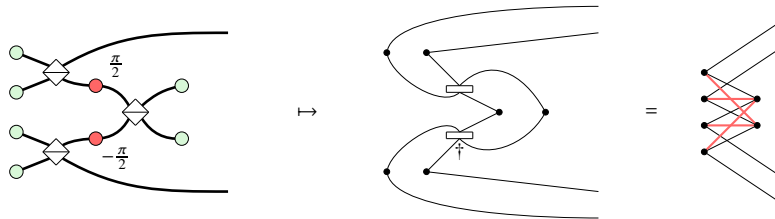
**Polarising beam splitters.** On bulk optics, the polarization states of photons can be acted upon using wave plates, polarizing beam splitters (PBSs) and photon counting measurements. Wave plates are simply  $X$  phase rotations, represented as red nodes in **ZX**. The PBS admits no description in **ZX**. It does however have a simple interpretation in **LO**:



In combination with  $X$  states and effects, polarising beam splitters can be used to perform post-selected fusion measurements and their transpose:

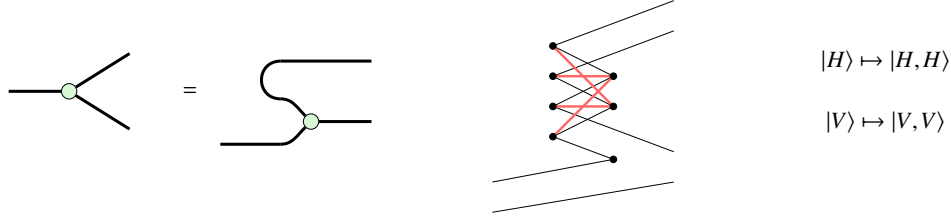


As an application, the linear-optical protocol for generating Bell states demonstrated in [13] may be described as a diagram using PBSs and ZX primitives:



We recover the diagram for the Bell state by reducing to normal form.

**Spiders.** The only missing ZX generator, which we need for a complete mapping  $\mathbf{ZX} \rightarrow \mathbf{QPath}$ , is the Z copy spider. We may readily deduce its representation using a known equality in ZX:



Similarly, we may turn the input leg into an output using a second Bell state. This yields a protocol for generating the dual-rail GHZ state using five ancillary photons. Note that the mapping is in no way unique, and we may obtain several equivalent protocols by further twisiting the spider above. This however increases the number of ancillary photons needed. As first shown in [14], any cluster state can be obtained by performing additional fusion measurements.

## Outlook

The theory in this paper is being implemented in DisCoPy [24], the Python library for monoidal categories. DisCoPy already has a number of tools for qubit quantum computing, including interfaces with tket [21], PyZX [22] and high-performance libraries for classical simulation. DisCoPy functors will allow to compile qubit circuits and cluster states into linear optical circuits for efficient simulation with Perceval [9] and future interfaces with photonic devices.

## Acknowledgements

The authors would like to thank Richie Yeung, Harny Wang, Douglas Brown, Alex Cowtan and Anna Pearson also from Quantinuum in Oxford, Alexis Toumi in Paris, Amar Hazihasanovic in Estonia, Lee Rozema and Iris Agresti in Vienna and Terry Rudolph from PsiQuantum in California, for the many conversations on optics which led to this manuscript and more to come.

## References

- [1] C. S. Wu and I. Shaknov. The Angular Correlation of Scattered Annihilation Radiation. *Physical Review*, 77(1):136–136, January 1950.
- [2] Alain Aspect, Jean Dalibard, and Gérard Roger. Experimental Test of Bell’s Inequalities Using Time-Varying Analyzers. *Physical Review Letters*, 49(25):1804–1807, December 1982.
- [3] D. Boschi, S. Branca, F. De Martini, L. Hardy, and S. Popescu. Experimental Realization of Teleporting an Unknown Pure Quantum State via Dual Classical and Einstein-Podolsky-Rosen Channels. *Physical Review Letters*, 80(6):1121–1125, February 1998.
- [4] A. R. Dixon, Z. L. Yuan, J. F. Dynes, A. W. Sharpe, and A. J. Shields. Gigahertz decoy quantum key distribution with 1 Mbit/s secure key rate. *Optics Express*, 16(23):18790–18797, November 2008.

- [5] Han-Sen Zhong, Hui Wang, Yu-Hao Deng, Ming-Cheng Cheng, Li-Chao Peng, Yi-Han Luo, Jian Qin, Dian Wu, Xing Ding, Yi Hu, Peng Hu, Xiao-Yan Yang, Wei-Jun Zhang, Hao Li, Yuxuan Li, Xiao Jiang, Lin Gan, Guangwen Yang, Lixing You, Zhen Wang, Li Li, Nai-Le Liu, Chao-Yang Lu, and Jian-Wei Pan. Quantum computational advantage using photons. *Science*, 370(6523):1460–1463, December 2020.
- [6] Scott Aaronson and Alex Arkhipov. The Computational Complexity of Linear Optics. *arXiv:1011.3245 [quant-ph]*, November 2010.
- [7] Giacomo Corrielli, Andrea Crespi, and Roberto Osellame. Femtosecond laser micromachining for integrated quantum photonics. 10(15):3789–3812.
- [8] Nathan Killoran, Josh Izaac, Nicolás Quesada, Ville Bergholm, Matthew Amy, and Christian Weedbrook. Strawberry fields: A software platform for photonic quantum computing. 3:129.
- [9] Nicolas Heurtel, Andreas Fyrrillas, Grégoire de Gliniasty, Raphaël Le Bihan, Sébastien Malherbe, Marceau Pailhas, Boris Bourdoncle, Pierre-Emmanuel Emeriau, Rawad Mezher, Luka Music, Nadia Belabas, Benoît Valiron, Pascale Senellart, Shane Mansfield, and Jean Senellart. Perceval: A Software Platform for Discrete Variable Photonic Quantum Computing. 2022.
- [10] E. Knill, R. Laflamme, and G. J. Milburn. A scheme for efficient quantum computation with linear optics. *Nature*, 409(6816):46–52, January 2001.
- [11] Michael A. Nielsen. Optical quantum computation using cluster states. *Physical Review Letters*, 93(4):040503, July 2004.
- [12] Pieter Kok, W. J. Munro, Kae Nemoto, T. C. Ralph, Jonathan P. Dowling, and G. J. Milburn. Review article: Linear optical quantum computing. *Reviews of Modern Physics*, 79(1):135–174, January 2007.
- [13] Qiang Zhang, Xiao-Hui Bao, Chao-Yang Lu, Xiao-Qi Zhou, Tao Yang, Terry Rudolph, and Jian-Wei Pan. Demonstration of efficient scheme for generation of "Event Ready" entangled photon pairs from single photon source. *Physical Review A*, 77(6):062316, June 2008.
- [14] Daniel E. Browne and Terry Rudolph. Resource-efficient linear optical quantum computation. *Physical Review Letters*, 95(1):010501, June 2005.
- [15] Sara Bartolucci, Patrick Birchall, Hector Bombin, Hugo Cable, Chris Dawson, Mercedes Gimeno-Segovia, Eric Johnston, Konrad Kieling, Naomi Nickerson, Mihir Pant, Fernando Pastawski, Terry Rudolph, and Chris Sparrow. Fusion-based quantum computation. *arXiv:2101.09310 [quant-ph]*, January 2021.
- [16] Samson Abramsky and Bob Coecke. A categorical semantics of quantum protocols. In *Proceedings of the 19th Annual IEEE Symposium on Logic in Computer Science (LICS)*, pages 415–425, March 2004.
- [17] P. Selinger. Dagger compact closed categories and completely positive maps. *Electronic Notes in Theoretical Computer Science*, 170:139–163, 2007.
- [18] B. Coecke, É. O. Paquette, and D. Pavlović. Classical and quantum structuralism. In S. Gay and I. Mackie, editors, *Semantic Techniques in Quantum Computation*, pages 29–69. Cambridge University Press, 2010. arXiv:0904.1997.
- [19] B. Coecke, R. Duncan, A. Kissinger, and Q. Wang. Strong complementarity and non-locality in categorical quantum mechanics. In *Proceedings of the 27th Annual IEEE Symposium on Logic in Computer Science (LICS)*, 2012. arXiv:1203.4988.
- [20] B. Coecke and A. Kissinger. *Picturing Quantum Processes. A First Course in Quantum Theory and Diagrammatic Reasoning*. Cambridge University Press, 2017.
- [21] Seyon Sivarajah, Silas Dilkes, Alexander Cowtan, Will Simmons, Alec Edgington, and Ross Duncan.  $\text{\texttt{t}\$}\text{\texttt{ket}\$}\text{\texttt{vangle}\$}$ : A retargetable compiler for NISQ devices. 6(1):014003.
- [22] Aleks Kissinger and John van de Wetering. PyZX: Large scale automated diagrammatic reasoning.
- [23] Dimitri Kartsaklis, Ian Fan, Richie Yeung, Anna Pearson, Robin Lorenz, Alexis Toumi, Giovanni de Felice, Konstantinos Meichanetzidis, Stephen Clark, and Bob Coecke. lambeq: An efficient high-level python library for quantum NLP.

- [24] Giovanni de Felice, Alexis Toumi, and Bob Coecke. DisCoPy: Monoidal Categories in Python. *arXiv:2005.02975 [math]*, May 2020.
- [25] E. R. Miranda, R. Yeung, A. Pearson, K. Meichanetzidis, and B. Coecke. A quantum natural language processing approach to musical intelligence. *arXiv preprint arXiv:2111.06741*, 2021.
- [26] Bob Coecke and Ross Duncan. Interacting Quantum Observables. In Luca Aceto, Ivan Damgård, Leslie Ann Goldberg, Magnús M. Halldórsson, Anna Ingólfssdóttir, and Igor Walukiewicz, editors, *Automata, Languages and Programming*, Lecture Notes in Computer Science, pages 298–310, Berlin, Heidelberg, 2008. Springer.
- [27] Ross Duncan, Aleks Kissinger, Simon Pedrix, and John van de Wetering. Graph-theoretic simplification of quantum circuits with the ZX-calculus.
- [28] Miriam Backens, Hector Miller-Bakewell, Giovanni de Felice, Leo Lobski, and John van de Wetering. There and back again: A circuit extraction tale. *Quantum*, 5:421, March 2021.
- [29] Niel de Beaudrap and Dominic Horsman. The ZX calculus is a language for surface code lattice surgery. 4:218.
- [30] Jamie Vicary. A categorical framework for the quantum harmonic oscillator. *International Journal of Theoretical Physics*, 47(12):3408–3447, December 2008.
- [31] M. Fiore. An axiomatization and a combinatorial model of creation/annihilation operators. *arXiv preprint arXiv:1506.06402*, 2015.
- [32] Leslie G. Valiant. Quantum computers that can be simulated classically in polynomial time. In *Proceedings of the Thirty-Third Annual ACM Symposium on Theory of Computing*, STOC '01, pages 114–123, New York, NY, USA, July 2001. Association for Computing Machinery.
- [33] Barbara M. Terhal and David P. DiVincenzo. Classical simulation of noninteracting-fermion quantum circuits. *Physical Review A*, 65(3):032325, March 2002.
- [34] Mario Krenn, Xuemei Gu, and Anton Zeilinger. Quantum Experiments and Graphs: Multiparty States as Coherent Superpositions of Perfect Matchings. *Physical Review Letters*, 119(24):240403, December 2017.
- [35] Stefan Ataman. A graphical method in quantum optics. 2(3):035032. Publisher: IOP Publishing.
- [36] R. F. Blute, Prakash Panangaden, and R. A. G. Seely. Fock Space: A Model of Linear Exponential Types, 1994.
- [37] Giovanni de Felice, Amar Hadzihasanovic, and Kang Feng Ng. A diagrammatic calculus of fermionic quantum circuits. *Logical Methods in Computer Science ; Volume 15*, page Issue 3 ; 18605974, 2019.
- [38] B. Coecke and A. Kissinger. The compositional structure of multipartite quantum entanglement. In *Automata, Languages and Programming*, Lecture Notes in Computer Science, pages 297–308. Springer, 2010. *arXiv:1002.2540*.
- [39] A. Hadzihasanovic. A Diagrammatic Axiomatisation for Qubit Entanglement. In *Proceedings of the 30th Annual ACM/IEEE Symposium on Logic in Computer Science*, LICS '15, pages 573–584. IEEE, 2015.
- [40] A. Hadzihasanovic. *The Algebra of Entanglement and the Geometry of Composition*. PhD thesis, University of Oxford, 2017.
- [41] Alexandre Clément and Simon Perdrix. PBS-calculus: A graphical language for quantum-controlled computations.
- [42] Paul McCloud. The category of linear optical quantum computing.
- [43] Alexandre Clément, Nicolas Heurtel, Shane Mansfield, Simon Perdrix, and Benoît Valiron. LOv-calculus: A graphical language for linear optical quantum circuits.
- [44] Hector Bombin, Chris Dawson, Ryan V. Mishmash, Naomi Nickerson, Fernando Pastawski, and Sam Roberts. Logical blocks for fault-tolerant topological quantum computation.
- [45] Francois Henault. Quantum physics and the beam splitter mystery. *arXiv:1509.00393 [quant-ph]*, page 95700Q, September 2015.



- [46] Michael Reck, Anton Zeilinger, Herbert J. Bernstein, and Philip Bertani. Experimental realization of any discrete unitary operator. *Physical Review Letters*, 73(1):58–61, July 1994.
- [47] William R. Clements, Peter C. Humphreys, Benjamin J. Metcalf, W. Steven Kolthammer, and Ian A. Walmsley. Optimal design for universal multiport interferometers. *Optica*, 3(12):1460–1465, December 2016.
- [48] David J Griffiths. *Introduction to electrodynamics*. Prentice Hall New Jersey, 1962.
- [49] Chris Heunen. On the functor  $\mathbb{I}^2$ . 7860:107–121.
- [50] John van de Wetering. ZX-calculus for the working quantum computer scientist.